

Numerical integration of the stochastic Landau-Lifshitz-Gilbert equation in generic time-discretisation schemes

Federico Romá^{1,2}, Leticia F. Cugliandolo² and Gustavo S. Lozano³

¹Departamento de Física, Universidad Nacional de San Luis & INFAP CONICET

Chacabuco 917, D5700BWS San Luis, Argentina

²Sorbonnes Universités, Université Pierre et Marie Curie - Paris 6

Laboratoire de Physique Théorique et Hautes Énergies UMR 7589

4, Place Jussieu, Tour 13, 5ème étage, 75252 Paris Cedex 05, France

³Departamento de Física, FCEYN Universidad de Buenos Aires & IFIBA CONICET

Pabellón 1 Ciudad Universitaria, 1428 Buenos Aires, Argentina

We introduce a numerical method to integrate the stochastic Landau-Lifshitz-Gilbert equation in spherical coordinates for generic discretisation schemes. This method conserves the magnetisation modulus and ensures the approach to equilibrium under the expected conditions. We test the algorithm on a benchmark problem: the dynamics of a uniformly magnetised ellipsoid. We investigate the influence of various parameters and, in particular, we analyse the efficiency of the numerical integration, in terms of the number of steps needed to reach a chosen long-time with a given accuracy.

I. INTRODUCTION

The design of magnetic devices used to store and process information crucially relies on a detailed understanding of how the magnetisation dynamics are influenced not only by external magnetic fields but also by dissipation and thermal fluctuations^{1,2}. In the simplest scenario, the time evolution of the magnetisation is governed by the stochastic generalisation of the Landau-Lifshitz-Gilbert (LLG) equation introduced by Brown to study of the relaxation of ferromagnetic nanoparticles³. In recent years, much attention has been directed to the theoretical and experimental understanding of how the magnetisation can be manipulated with spin polarized currents via the spin torque effect originally discussed by Slonczewski⁴ and Berger⁵, an effect that can be described by a simple generalisation of this equation.

Explicit analytical solutions to the stochastic Landau-Lifshitz-Gilbert equation are available in very few cases; in more general circumstances information has to be obtained by direct numerical simulation of the stochastic equation, the study of the associated Fokker-Planck equation (see Ref. 6 for a recent review), or via functional methods⁷.

The stochastic LLG equation is a stochastic equation with *multiplicative* noise. It is a well-known fact that in these cases, a careful analysis of the stochastic integration prescriptions is needed to preserve the physical properties of the model. In the stochastic Landau-Lifshitz-Gilbert case one should force the modulus of the magnetisation to stay constant during evolution, and different schemes (Ito, Stratonovich or the generic ‘alpha’ prescription) require the addition of different drift terms to preserve this property (for a recent discussion see Ref. 7). All these issues are by now well-understood and they are also easy to in the continuous time treatment of the problem. Nevertheless, this problem has not been analysed in so much detail in the numerical formulation of the equation.

Indeed, most of the works focusing on the numerical analysis of the stochastic equation use Cartesian coordinates^{8–18}. Although there is nothing fundamentally wrong with this coordinate system, most algorithms based on it do not preserve, in an automatic way, the norm of the magnetisation during time evolution. These algorithms require the explicit magnetisation normalisation after every time step, a trick that is often hidden behind other technical difficulties^{19,20}. This problem can be avoided only if the specific midpoint prescription (Stratonovich) is used¹³.

Given that the modulus of the magnetisation should be constant by construction, a more convenient way to describe the time evolution should be to use the spherical coordinate system. Despite its naturalness, no detailed analysis of this case exists in the literature. The aim of this work is to present a numerical algorithm to solve the LLG equation in the spherical coordinates system and to discuss in detail how different discretisation prescriptions are related, an issue which is not trivial due to the multiplicative character of the thermal noise.

In order to make precise statements, we will focus on the study the low-temperature dynamics of an ellipsoidal Cobalt nano particle, a system that has been previously studied in great detail by other groups¹³. The paper is organised as follows. In Sec. II we present the problem. We first recall the stochastic Landau-Lifshitz-Gilbert equation in Cartesian and spherical coordinates. In both cases we discuss the drift term needed to ensure the conservation of the magnetisation modulus as well as the approach to Boltzmann equilibrium. We then describe the concrete problem that we will solve numerically. In Sec. III we present the numerical analysis. We first introduce the algorithm and we then discuss the results. Section IV is devoted to the conclusions.

II. THE PROBLEM

A. The stochastic Landau-Lifshitz-Gilbert equation

The stochastic Landau-Lifshitz-Gilbert (sLLG) equation in the Landau formulation of dissipation²¹ reads

$$d_t \mathbf{M} = -\frac{\gamma_0}{1 + \gamma_0^2 \eta^2} \mathbf{M} \wedge \left(\mathbf{H}_{\text{eff}} + \mathbf{H} + \frac{\eta \gamma_0}{M_s} \mathbf{M} \wedge (\mathbf{H}_{\text{eff}} + \mathbf{H}) \right), \quad (1)$$

where $d_t \equiv d/dt$. $\gamma_0 \equiv \gamma \mu_0$ is the product of γ , the gyromagnetic ratio relating the magnetisation to the angular momentum, and μ_0 , the vacuum permeability constant. The gyromagnetic factor is given by $\gamma = \mu_B g / \hbar$ and in our convention $\gamma > 0$ with μ_B Bohr's magneton and g Lande's g -factor. The symbol \wedge denotes a vector product. For $\mathbf{H} = 0$ the first term in the right-hand-side describes the magnetisation precession around the local effective magnetic field \mathbf{H}_{eff} . The term proportional to $\mathbf{M} \wedge (\mathbf{M} \wedge \mathbf{H}_{\text{eff}})$ is responsible for dissipation. Thermal effects are introduced à la Brown via the random field \mathbf{H}^3 that is

assumed to be Gaussian distributed with average and correlations

$$\langle H_i(t) \rangle_{\mathbf{H}} = 0, \quad \langle H_i(t) H_j(t') \rangle_{\mathbf{H}} = 2D \delta_{ij} \delta(t - t'), \quad (2)$$

for all $i, j = x, y, z$. The parameter D is, for the moment, free and will be determined below. η is the dissipation coefficient and in most relevant physical applications, $\gamma_0 \eta \ll 1$. An equivalent way of introducing dissipation was proposed by Gilbert²² but we have chosen to work with the Landau formalism in this work.

Due to the multiplicative character of the noise, the above equation conserves the modulus of \mathbf{M} and takes to Boltzmann equilibrium *only if* the Stratonovich, mid-point prescription, stochastic calculus is used. Otherwise, for other stochastic discretisation prescriptions, none of these physically expected properties are ensured. The addition of a carefully chosen drift term is needed to recover the validity of these properties when other stochastic calculus are used. The generic modified sLLG equation⁷

$$D_t^{(\alpha)} \mathbf{M} = -\frac{\gamma_0}{1 + \gamma_0^2 \eta^2} \mathbf{M} \wedge \left(\mathbf{H}_{\text{eff}} + \mathbf{H} + \frac{\eta \gamma_0}{M_s} \mathbf{M} \wedge (\mathbf{H}_{\text{eff}} + \mathbf{H}) \right), \quad (3)$$

where the time-derivative has been replaced by the α -covariant derivative

$$D_t^{(\alpha)} = d_t + 2D(1 - 2\alpha) \frac{\gamma_0^2}{1 + \eta^2 \gamma_0^2}, \quad (4)$$

ensures the conservation of the magnetisation modulus for any value of D . On top, having modified the stochastic equation in this way, one easily proves that the associated Fokker-Planck equation is independent of α and takes the magnetisation to its equilibrium Boltzmann distribution at temperature T provided the parameter D be given by

$$D = \frac{\eta k_B T}{M_s V \mu_0}, \quad (5)$$

where V is the volume of the sample that behaves as a single macrospin, k_B the Boltzmann constant, and M_s is the saturation magnetisation. The parameter α is constrained to vary in $[0, 1]$. The most popular conventions are the Itô one that corresponds to $\alpha = 0$ and the Stratonovich calculus that is defined by $\alpha = 1/2$.

As the modulus of the magnetisation is conserved, this problem admits a more natural representation in spherical coordinates. The vector \mathbf{M} defines the usual local basis $(\mathbf{e}_r, \mathbf{e}_\theta, \mathbf{e}_\phi)$ with

$$\mathbf{M}(M_s, \theta, \phi) \equiv M_s \mathbf{e}_r(\theta, \phi) \quad (6)$$

and

$$\begin{aligned}
M_x(t) &= M_s \sin \theta(t) \sin \phi(t) , \\
M_y(t) &= M_s \sin \theta(t) \cos \phi(t) , \\
M_z(t) &= M_s \cos \theta(t) .
\end{aligned} \tag{7}$$

The sLLG equation in this system of coordinates becomes⁷

$$d_t M_s = 0 , \tag{8}$$

$$\begin{aligned}
d_t \theta &= \frac{D(1-2\alpha)\gamma_0^2}{1+\eta^2\gamma_0^2} \cot \theta \\
&\quad + \frac{\gamma_0}{1+\eta^2\gamma_0^2} [H_{\text{eff},\phi} + H_\phi + \eta\gamma_0(H_{\text{eff},\theta} + H_\theta)] ,
\end{aligned} \tag{9}$$

$$\sin \theta \, d_t \phi = \frac{\gamma_0}{1+\eta^2\gamma_0^2} [\eta\gamma_0(H_{\text{eff},\phi} + H_\phi) - (H_{\text{eff},\theta} + H_\theta)] , \tag{10}$$

where the θ and ϕ components of the stochastic field are defined as

$$H_\theta = H_x \cos \theta \cos \phi + H_y \cos \theta \sin \phi - H_z \sin \theta , \tag{11}$$

$$H_\phi = -H_x \sin \phi + H_y \cos \phi , \tag{12}$$

and similarly for \mathbf{H}_{eff} .

We introduce an adimensional time, $\tau = \gamma_0 M_s t$, the adimensional damping constant $\eta_0 = \eta\gamma_0$, and we normalise the field and the magnetisation by M_s defining, $\mathbf{m} = \mathbf{M}/M_s$, $\mathbf{h}_{\text{eff}} = \mathbf{H}_{\text{eff}}/M_s$, $\mathbf{h} = \mathbf{H}/M_s$, to write the equations as

$$\begin{aligned}
d_\tau \theta &= \frac{D\gamma_0(1-2\alpha)\gamma_0}{M_s(1+\eta_0^2)} \cot \theta \\
&\quad + \frac{1}{1+\eta_0^2} [h_{\text{eff},\phi} + h_\phi + \eta_0(h_{\text{eff},\theta} + h_\theta)] ,
\end{aligned} \tag{13}$$

$$\sin \theta \, d_\tau \phi = \frac{1}{1+\eta_0^2} [\eta_0(h_{\text{eff},\phi} + h_\phi) - (h_{\text{eff},\theta} + h_\theta)] . \tag{14}$$

The random field statistics is now modified to $\langle h_i(\tau) \rangle = 0$ and $\langle h_i(\tau) h_j(\tau') \rangle = 2D\gamma_0/M_s \, \delta_{ij} \, \delta(\tau - \tau')$.

B. The benchmark

We focus here on the dynamics of a uniformly magnetised ellipsoid with energy per unit volume

$$U = -\mu_0 \mathbf{M} \cdot \mathbf{H}_{\text{ext}} + \frac{\mu_0}{2} (d_x M_x^2 + d_y M_y^2 + d_z M_z^2) . \tag{15}$$

\mathbf{H}_{ext} is the external magnetic field and d_x , d_y , d_z are the anisotropy parameters. This case has been analysed in detail in Ref. 13 and will be used as a benchmark to compare our results. We normalise the energy density by $\mu_0 M_s^2$, and write

$$u = -\mathbf{m} \cdot \mathbf{h}_{\text{ext}} + \frac{1}{2}(d_x m_x^2 + d_y m_y^2 + d_z m_z^2) . \quad (16)$$

The effective magnetic field is $\mathbf{H}_{\text{eff}} = -\mu_0^{-1} \partial U / \partial \mathbf{M}$. Once normalised by M_s , it reads

$$\mathbf{h}_{\text{eff}} = \mathbf{h}_{\text{ext}} - (d_x m_x \mathbf{e}_x + d_y m_y \mathbf{e}_y + d_z m_z \mathbf{e}_z) . \quad (17)$$

We will study the dynamics of a Cobalt nano particle of prolate spherical form with radii $c = 4$ [nm] (in the z easy-axis direction) and $a = b = 2$ [nm] (in the x and y directions, respectively), yielding a volume $V = 6.702 \times 10^{-26}$ [m³]. There is no external applied field, the saturation magnetisation is $M_s = 1.42 \times 10^6$ [A/m], the uniaxial anisotropy constant in the z direction is $K_1 = 10^5$ [J/m³], and the temperature is $T = 300$ [K]. In the following we will work with the adimensional damping constant $\eta_0 = \eta \gamma_0$ and the physical value for it is $\eta_0 = 0.005$. For these nano particle one has $d_x = N_x = d_y = N_y = 0.4132$ (where N_i are the demagnetisation factors²⁴), and $d_z = N_z - 2K_1/(\mu_0 M_s^2) = 0.0946$ since $N_z = 0.1736$. The constant γ_0 takes the value 2.21276157×10^5 [m/(As)]. We recall here that in Ref. 13 the time-step used in the numerical integration is $\Delta t = 1.6$ [ps], that is equivalent to $\Delta \tau = (\gamma_0 M_s) \Delta t = 0.5$.

For future reference, we mention here that in the absence of an external field, $\mathbf{h}_{\text{ext}} = 0$, the energy density u can be written in terms of the z component of the magnetisation as

$$u = \frac{1}{2} [d_x (1 - m_z^2) + d_z m_z^2] . \quad (18)$$

III. NUMERICAL ANALYSIS

In this Section we first give some details on the way in which we implemented the numerical code that integrates the equations, and we next present our results.

A. Method

First, we stress an important fact already explained in Ref. 7: the random fields h_θ and h_ϕ are not Gaussian white noises but acquire, due to the pre factors that depend on the angles,

a more complex distribution function. Therefore, we will not draw these random numbers but the original Cartesian components of the random field that are uncorrelated Gaussian white noises. We then recover the field h_θ and h_ϕ by using Eqs. (11) and (12) and the time-discretisation of the product explained below. Most methods used to integrate the sLLG equation rely on explicit schemes. Such are the cases of the Euler and Heun methods. While the former converge to the Ito solution, the latter lead to the Stratonovich limit⁸. To preserve the module of \mathbf{m} , in these algorithms it is necessary to normalise the magnetisation in each step, a nonlinear modification of the original sLLG dynamics²⁰. Implicit schemes, on the other hand, are very stable and, for example, the mid-point method (Stratonovich stochastic calculus) provides a simple way to automatically preserve the module under discretisation¹³. In what follows, we describe our numerical-implicit scheme which keeps the module length constant and, unlike previous approaches, it is valid also for any discretisation prescriptions.

Next, we define the α -prescription angular variables according to

$$\theta^\alpha(\tau) \equiv \alpha\theta(\tau + \Delta\tau) + (1 - \alpha)\theta(\tau) , \quad (19)$$

$$\phi^\alpha(\tau) \equiv \alpha\phi(\tau + \Delta\tau) + (1 - \alpha)\phi(\tau) , \quad (20)$$

with $0 \leq \alpha \leq 1$. In the following we use the short-hand notation $\theta^\alpha(\tau) = \theta_\tau^\alpha$, $\theta(\tau) = \theta_\tau$ and so on and so forth. The discretised dynamic equations now read $F_\theta = 0$ and $F_\phi = 0$ with

$$\begin{aligned} F_\theta \equiv & -(\theta_{\tau+\Delta\tau} - \theta_\tau) + D_0 \Delta\tau \frac{(1 - 2\alpha)}{(1 + \eta_0^2)} \cot \theta_\tau^\alpha , \\ & + \frac{\Delta\tau}{1 + \eta_0^2} [h_{\text{eff},\phi}^\alpha + \eta_0 h_{\text{eff},\theta}^\alpha] + \frac{1}{1 + \eta_0^2} [\Delta W_\phi + \eta_0 \Delta W_\theta] , \end{aligned} \quad (21)$$

$$\begin{aligned} F_\phi \equiv & -(\phi_{\tau+\Delta\tau} - \phi_\tau) \\ & + \frac{\Delta\tau}{1 + \eta_0^2} \left[\frac{\eta_0 h_{\text{eff},\phi}^\alpha - h_{\text{eff},\theta}^\alpha}{\sin \theta_\tau^\alpha} \right] + \frac{1}{1 + \eta_0^2} \left[\frac{\eta_0 \Delta W_\phi - \Delta W_\theta}{\sin \theta_\tau^\alpha} \right] , \end{aligned} \quad (22)$$

where $D_0 = D\gamma_0/M_s$ and the effective fields at the α -point are $h_{\text{eff},\theta}^\alpha \equiv h_{\text{eff},\theta}(\theta_\tau^\alpha, \phi_\tau^\alpha)$ and $h_{\text{eff},\phi}^\alpha \equiv h_{\text{eff},\phi}(\theta_\tau^\alpha, \phi_\tau^\alpha)$.

The numerical integration of the discretised dynamics consists in finding the roots of the coupled system of equations $F_\theta = 0$ and $F_\phi = 0$ with the left-hand-sides given in Eqs. (21) and (22). We used a Newton-Raphson routine²³ and we imposed that the quantity $F_\theta^2 + F_\phi^2$ be smaller than 10^{-10} . (To avoid singular behaviour when the magnetisation gets too close to the z axis, $\theta = 0$ or $\theta = \pi$, we apply in these cases a $\pi/2$ -rotation of the coordinate system around the y axis.)

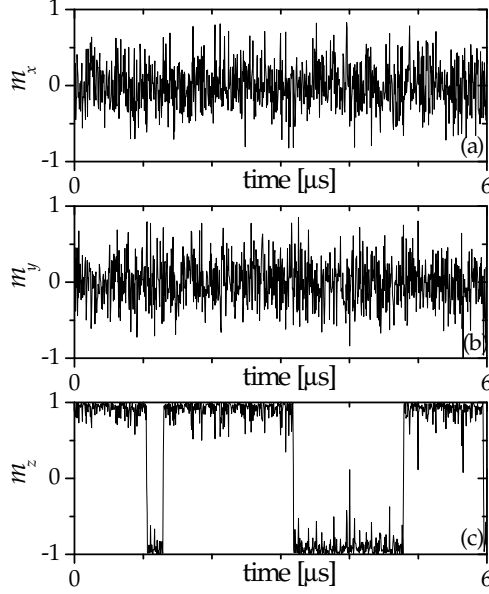


FIG. 1. A typical magnetisation trajectory as a function of real time measured in μs showing rapid fluctuations around zero for m_x (a) and m_y (b) and telegraphic noise with sudden transitions between the up and down magnetisation configurations for m_z (c). The initial condition is $\mathbf{m} = (0, 0, 1)$, $\alpha = 0.5$, $\eta_0 = 0.005$, $\Delta\tau = 0.5$, and $\tau_{max} = 2 \times 10^6$ that is equivalent to $t_{max} = 6.36 \mu\text{s}$. In this and all other figures the working temperature is $T = 300 \text{ K}$.

All the results we will present below, averages and distributions, have been computed using 10^5 independent runs.

B. Results

1. Stratonovich calculus

We start by using the Stratonovich discretisation scheme, $\alpha = 0.5$, to numerically integrate the stochastic equation using the parameters listed in Sec. II B that are the same as the ones used in Ref. 13. We simply stress here that these are typical parameters (in particular, notice the small value of the damping coefficient η_0). Although we solved the problem in spherical coordinates, we illustrate our results in cartesian coordinates (using back Eqs. 7) to allow for an easier comparison with existing literature.

a. Trajectories. Figure 1 displays the three Cartesian components of the magnetisation, m_x , m_y , m_z , as a function of time for a single run starting from an initial condition

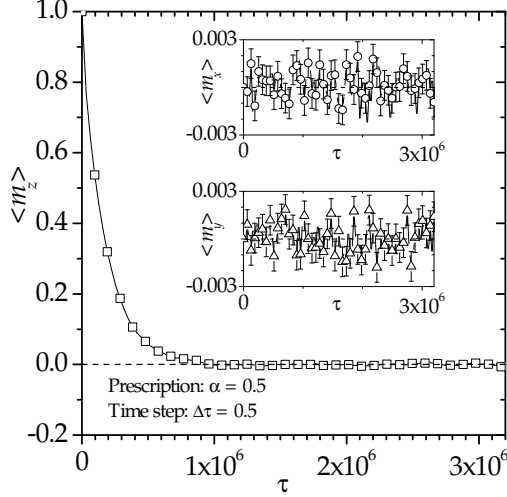


FIG. 2. Average value of the magnetisation z -component as a function of τ . Insets: τ -dependence of the other two components, $\langle m_x \rangle$ and $\langle m_y \rangle$. $\alpha = 0.5$, $\eta_0 = 0.005$, and $\Delta\tau = 0.5$.

that is perfectly polarised along the z axis, $\mathbf{m} = (0, 0, 1)$. The data show that while the x and y components fluctuate around zero, the z component has telegraphic noise, due to the very fast magnetisation reversal from the ‘up’ to the ‘down’ position and vice versa. Indeed, the working temperature we are using is rather low but sufficient to drive such transitions.

b. Equilibrium criteria. In Fig. 2 we show the relaxation of the thermal average of the z component, $\langle m_z \rangle$, evolving from the totally polarised initial condition, $\mathbf{m} = (0, 0, 1)$, during a maximum adimensional time $\tau_{max} = 3.2 \times 10^6$. In the inset one can see temporal fluctuations around zero in the averages of the two other components, $\langle m_x \rangle$ and $\langle m_y \rangle$. The error bars in these and other plots are estimated as one standard deviation from the data-average, and when these are smaller than the data points we do not include them in the plots. The data in the main panel demonstrate that for times shorter than 10^6 the system is still out of equilibrium while for longer times this average is very close to the equilibrium expectation, $\langle m_z \rangle_{eq} = 0$.

A more stringent test of equilibration is given by the analysis of the probability distribution function (pdf) of the three Cartesian components m_x , m_y , m_z . In Fig. 3 (a) we present the numerical pdfs of m_z , $P(m_z)$, and we compare the numerical data to the theoretical distribution function in equilibrium. We computed the former by sampling over the second half of the temporal window, that is to say, by constructing the histogram with data

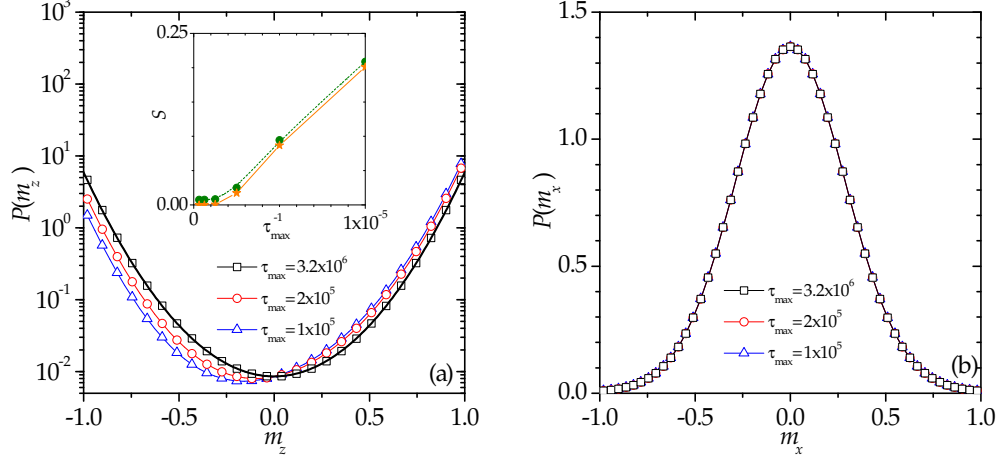


FIG. 3. (Colour online.) (a) $P(m_z)$, in a linear-log scale, obtained as explained in the main text for three values of τ_{max} given in the key compared to the exact equilibrium law (continuous line). The inset shows the parameter S defined in Eq. (25) as a function of τ_{max}^{-1} . The upper curve has been computed using the exact pdf $P_{eq}(m_z)$ while the lower one, that gets closer to zero, has been computed using a finite number of bins to approximate the exact $P_{eq}(m_z)$. (b) $P(m_x)$, in a double linear scale, for the same runs. $\alpha = 0.5$, $\eta_0 = 0.005$, and $\Delta\tau = 0.5$.

collected over $\tau_{max}/2 \leq \tau \leq \tau_{max}$, and then averaging the histograms over 10^5 independent runs. For the equilibrium $P_{eq}(m_z)$ we note that the equilibrium probability density of the spherical angles is

$$P_{eq}(\theta, \phi) d\theta d\phi \propto \frac{1}{4\pi} \sin \theta e^{-\varepsilon u} d\theta d\phi, \quad (23)$$

where $\varepsilon = \mu_0 M_s^2 V / (k_B T)$, that implies

$$P_{eq}(m_z) dm_z = -\frac{1}{2} e^{-\varepsilon u} dm_z = \frac{1}{Z} e^{-\frac{\varepsilon}{2}[d_x(1-m_z^2)+d_z m_z^2]} dm_z. \quad (24)$$

For the parameters used in the simulation $\varepsilon = 41$ and $Z = 0.0244$. It is quite clear from Fig. 3 that the numerical curves for the two shortest τ_{max} are still far from the equilibrium one, having excessive weight on positive values of m_z . The last curve, obtained for the longest running time, $\tau_{max} = 3.2 \times 10^6$ is, on the contrary, indistinguishable from the equilibrium one in this presentation. A more quantitative comparison between numerical and analytic pdfs is given in the inset of Fig. 3 (a) where the probability distribution ‘H-function’²⁵

$$S(\tau_{max}) = \int_{-1}^1 dm_z P(m_z, \tau_{max}) \ln \frac{P(m_z, \tau_{max})}{P_{eq}(m_z)}, \quad (25)$$

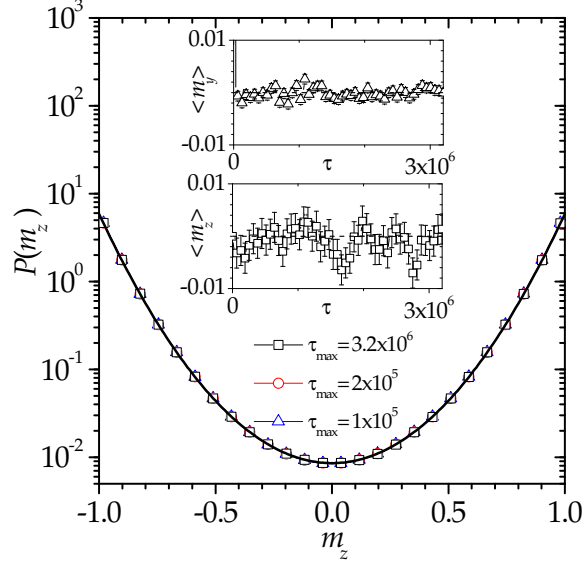


FIG. 4. (Colour online.) $P(m_z)$, in a linear-log scale, for three values of τ_{max} given in the key, compared to the exact equilibrium law (continuous line). The insets show the averages of $\langle m_y \rangle$ and $\langle m_z \rangle$ as a function of τ . The parameters are the same as in Fig. 2 but the initial condition is $\mathbf{m} = (0, 1, 0)$.

with $P_{eq}(m_z)$ given in Eq. (24), is plotted as a function of inverse time τ_{max}^{-1} . The two sets of data in the inset correspond to S computed with the continuous analytic form (24), data falling above, and with a discretised version of it where the same number of bins as in the numerical simulation are used (concretely, 51), data falling below and getting very close to zero for the longest τ_{max} used. The latter is the correct way of comparing analytic and numerical data and yields, indeed, a better agreement with what was expected. Finally, in panel (b) we show the pdf of m_x for the same three τ_{max} used in panel (a), and we observe a faster convergence to an equilibrium distribution with a form that is very close to a Gaussian. For symmetry reasons the behaviour of m_y is the same.

Figure 4 shows the pdfs for the same set of parameters but starting from the initial condition $\mathbf{m} = (0, 1, 0)$. The approach to equilibrium is faster in this case: all curves fall on top of the theoretical one. The insets are for the time-dependence of $\langle m_x \rangle$ and $\langle m_z \rangle$ that still fluctuate around zero with larger temporal fluctuations for the latter than the former. We reckon here that the fluctuations of $\langle m_y \rangle$ and $\langle m_z \rangle$ are quite different. The oscillations of $\langle m_z \rangle$ around zero are due to the telegraphic noise of this component and to the fact that

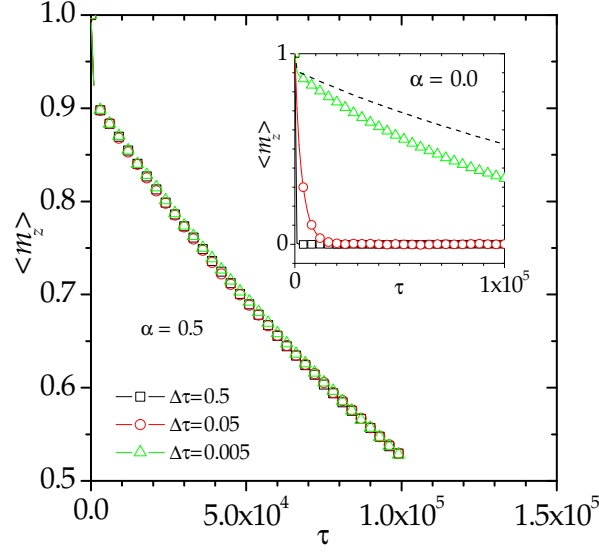


FIG. 5. (Colour online.) $\langle m_z \rangle$ as a function of τ for $\alpha = 0.5$, $\eta_0 = 0.005$ and $\Delta\tau = 0.5, 0.05$ and 0.005 . The inset shows $\langle m_z \rangle$ against τ for $\alpha = 0.0$ and the same $\Delta\tau$ with the same symbol code as in the main part of the figure. The dotted black line is a reference and corresponds to $\alpha = 0.5$ and $\Delta\tau = 0.005$. The initial condition is $\mathbf{m} = (0, 0, 1)$.

the average is done over a finite number of runs. The amplitude of these oscillations tend to zero with an increasing number of averages.

We conclude this analysis by stating that the dynamics in the spherical coordinate system for the Stratonovich discretisation scheme behave correctly, with the advantage of keeping the norm of the magnetisation fixed by definition.

2. Generic calculus

Although it was shown in Ref. 7 that in the $\Delta\tau \rightarrow 0$ limit every discretisation of the stochastic equation leads to equilibrium, the numerical integration of the equations is done at finite $\Delta\tau$ and the time-dependent averaged observables may depend on $\Delta\tau > 0$. With this in mind, we investigated which discretisation scheme is more efficient in terms of computational effort. The aim of this section is to study the $\Delta\tau$ dependence of the numerical results for different values of α and to determine for which α one can get closer to the continuous time limit ($\Delta\tau \rightarrow 0$) for larger values of $\Delta\tau$.

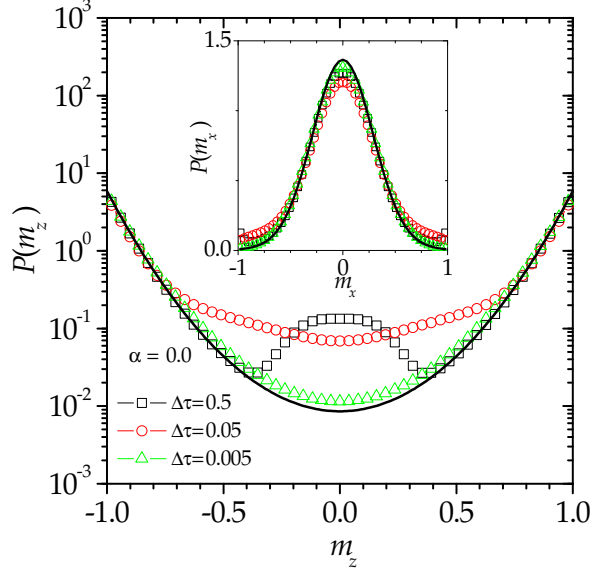


FIG. 6. (Colour online.) $P(m_z)$ for $\alpha = 0.0$, $\eta_0 = 0.005$ and $\Delta\tau = 0.5, 0.05$ and 0.005 , compared to the exact equilibrium law (continuous line). The initial condition is $\mathbf{m} = (0, 1, 0)$. The inset shows the distributions $P(m_x)$ for the same runs and using the same symbol code as in the main part of the figure, compared to the limit (equilibrium) function shown in Fig. 3 (b) for $\alpha = 0.5$ and the longest τ_{max} .

For Stratonovich calculus, i.e. for $\alpha = 0.5$, we reckon that the time-dependent results do not depend strongly on $\Delta\tau$ for $\Delta\tau \leq 0.5$ (see the main panel of Fig. 5 where data for $\Delta\tau = 0.005, 0.05, 0.5$ prove this claim) and we can assert that the master curve is as close as we can get, for the numerical accuracy we are interested in, to the one for $\Delta\tau \rightarrow 0$, that is to say, to the correct relaxation. Instead, for other discretisation prescriptions, the dependence on $\Delta\tau$ is stronger. For example, for $\alpha = 0$ (Ito calculus) the curves for $\Delta\tau = 0.05$ and 0.005 are still notably different from each other, see the insert to Fig. 5, and they have not yet converged to the physical time-dependent average. Even smaller values of $\Delta\tau$ are needed to get close to the asymptotically correct relaxation, shown with a black dotted line. We do not show the pdfs here but, consistently, they are far away from the equilibrium one for these values of $\Delta\tau$.

In Fig. 6 we use the initial condition $\mathbf{m} = (0, 1, 0)$ to see whether the efficiency of the Ito calculus improves in this case. Although the values of $\langle m_z \rangle$ are very close to the expected

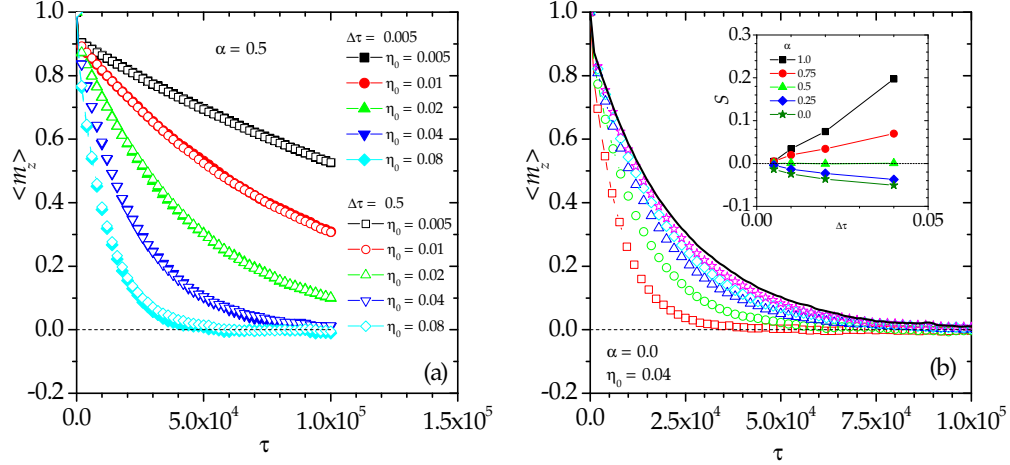


FIG. 7. (Colour online.) (a) Comparison between $\langle m_z \rangle$ against τ for two values of the time-increment, $\Delta\tau = 0.5$ (open symbols) and 0.005 (filled symbols). $\alpha = 0.5$ and several values of the damping coefficient η_0 (shown with different colours) as written in the key. (b) Ito calculus, $\alpha = 0$, and $\eta_0 = 0.04$. Curves correspond to $\tau_{max} = 10^5$ and different $\Delta\tau = 0.005, 0.01, 0.02, 0.04, 0.08$ (from top to bottom). The continuous line displays $\langle m_z \rangle$ for $\alpha = 0.5$, $\eta_0 = 0.04$ and $\Delta\tau = 0.005$. Inset: the parameter S defined in Eq. (26) for these curves taking as a reference the curve for $\alpha = 0.5$.

vanishing value both distributions, $P(m_z)$ (main panel) and $P(m_x)$ (inset), are still far from equilibrium. We conclude that also for this set of initial conditions smaller $\Delta\tau$ are needed to reach the continuous time limit. We have investigated other values of $\alpha \neq 0.5$ and in all cases we have found that convergence is slower than for the $\alpha = 0.5$ case.

We conclude that the Stratonovich calculus is ‘more efficient’ than all other α -prescriptions in the sense that one can safely use larger values of $\Delta\tau$ (and therefore reach longer times) in the simulation. This does not mean that other discretisation schemes yield incorrect results. For $\alpha \neq 0.5$ one must use smaller values of the time-step $\Delta\tau$ to obtain the physical behaviour.

3. Effect of the damping coefficient

Intuitively, one knows that the relaxation should be faster for larger values of the damping coefficient η_0 . In this Section we progressively increase η_0 (towards unphysical values) to

check whether the strong $\Delta\tau$ dependence found for the $\alpha \neq 0.5$ calculus remains under strong dissipation.

In Fig. 7 (a) we test the $\Delta\tau$ dependence of $\langle m_z \rangle$ for $\alpha = 0.5$ and five values of η_0 ranging from $\eta_0 = 0.005$ to $\eta_0 = 0.08$ and increasing by a factor of two. Filled and open data points with the same colour correspond to $\Delta\tau = 0.005$ and $\Delta\tau = 0.5$, respectively. The agreement between the two data sets is very good for all η_0 . Indeed the agreement is so good that data are superimposed and it is hard to distinguish the different cases. The curves also show that the dynamics are faster for increasing η_0 . Figure 7 (b) displays the decay of $\langle m_z \rangle$ as a function of time for $\alpha = 0$ and a rather large value of the damping coefficient, $\eta_0 = 0.04$, for different time increments, $\Delta\tau = 0.005, 0.01, 0.02, 0.04, 0.08$. The curves tend to approach the reference one shown with a continuous line and corresponding to $\alpha = 0.5$ for decreasing values of $\Delta\tau$. A quantitative measure of the convergence rate is given by another S parameter, defined as

$$S(\Delta\tau, \alpha) = \frac{1}{\tau_{max}} \int_0^{\tau_{max}} d\tau \langle m_z \rangle_\alpha \ln \left[\frac{\langle m_z \rangle_\alpha}{\langle m_z \rangle_{0.5}} \right], \quad (26)$$

and shown in the inset for $\eta_0 = 0.04$. Here, $\langle m_z \rangle_{0.5}$ is the average of m_z for $\alpha = 0.5$ and $\Delta\tau = 0.005$, while $\langle m_z \rangle_\alpha$ is the curve corresponding to other values of α and $\Delta\tau$. For all α -schemes S tends to zero for $\Delta\tau \rightarrow 0$. Note that for $\alpha = 0.5$ this parameter is very close to zero for all the $\Delta\tau$ values shown in the figure, a confirmation of the fact that this prescription yields very good results for relatively large values of $\Delta\tau$ and it is therefore ‘more efficient’ computationally.

IV. CONCLUSIONS

In this paper we introduced a numerical algorithm that solves the the sLLG dynamic equation in the spherical coordinate system with no need for artificial normalisation of the magnetisation. We checked that the algorithm yields the correct evolution of a simple and well-documented problem¹³, the dynamics of an ellipsoidal magnetic nano-particle. We applied the algorithm in the generic ‘alpha’-discretisation prescription. We showed explicitly how the finite $\Delta\tau$ dynamics depend on α , despite the fact that the final equilibrium distribution is α -independent. We showed that at least for the case reported here, the Stratonovich mid-point prescription is the ‘more efficient one’ in the sense that the dependence of the

dynamics on the finite value of $\Delta\tau$ is less pronounced so, larger values of $\Delta\tau$ can be used to explore the long time dynamics. We think it would be worth to explore, both analytically and numerically, if this is a generic result of the sLLG dynamics. We hope to report on this issue in the near future.

Acknowledgements. We thank C. Aron, D. Barci and Z. González-Arenas for very helpful discussions on this topic. FR acknowledges financial support from CONICET (PIP 114-201001-00172) and Universidad Nacional de San Luis, Argentina (PROIPRO 31712) and thanks the LPTHE for hospitality during the preparation of this work. LFC & GSL acknowledge financial support from PICT-2008-0516 (Argentina).

REFERENCES

- ¹B. Hillebrands and K. Ounadjela, eds. *Spin dynamics in confined magnetic structures* (Springer, Berlin, 2002).
- ²G. Bertotti, I. Mayergoyz, and C. Serpico, *Nonlinear magnetization dynamics in nanosystems* (Elsevier, Amsterdam, 2009).
- ³W. F. Brown, Phys. Rev. **130**, 1677 (1963).
- ⁴J. C. Slonczewski, J. Magn. Magn. Mat. **159**, L1 (1996).
- ⁵L. Berger, Phys. Rev. B **54**, 9353 (1996).
- ⁶Thermal fluctuations of magnetic nanoparticles: Fifty years after Brown Coffey, William T. and Kalmykov, Yuri P. Journal of Applied Physics **112**, 121301 (2012)
- ⁷C. Aron, D. G. Barci, L. F. Cugliandolo, Z. González Arenas, and G. S. Lozano, arXiv:1402.1200.
- ⁸J. L. García-Palacios and F. J. Lázaro, Phys. Rev. B **58**, 14937 (1998).
- ⁹U. Nowak, R. W. Chantrell, and E. C. Kennedy, Phys. Rev. Lett. **84**, 163 (2000).
- ¹⁰Z. Li and S. Zhang, Phys. Rev. B **69**, 134416 (2004).
- ¹¹X. Z. Cheng, M. B. A. Jalil, H. K. Lee, and Y. Okabe, Phys. Rev. B **72**, 094420 (2005).
- ¹²X. Z. Cheng, M. B. A. Jalil, H. K. Lee, and Y. Okabe, Phys. Rev. Lett. **96**, 067208 (2006).
- ¹³M. d’Aquino, C. Serpico, G. Coppola, I. D. Mayergoyz, and G. Bertotti, J. of Appl. Phys. **99**, 08B905 (2006).
- ¹⁴K. D. Usadel, Phys. Rev. B **73**, 212405 (2006).

- ¹⁵N. Kazantseva *et al.*, Phys. Rev. B **77**, 184428 (2008).
- ¹⁶S. V. Titov and P. M. Déjardin, H. El Mrabti, and Y. P. Kalmykov, Phys. Rev. B **82**, 100413 (2010).
- ¹⁷M. Weiler *et al.*, Phys. Rev. Lett. **106**, 117601 (2011).
- ¹⁸C. Haase and U. Nowak, Phys. Rev. B **85**, 045435 (2012).
- ¹⁹E. Martínez, L. López-Díaz, L. Torres, and O. Alejos, Physica B **343**, 252 (2004).
- ²⁰I. Cimrák, Arch. Comput. Meth. Eng. **15**, 1 (2007).
- ²¹L. D. Landau and E. M. Lifshitz, Phys. Z. Sowietunion **8**, 153 (1935).
- ²²T. L. Gilbert, Phys. Rev. **100**, 1243 (1955). T. L. Gilbert, IEEE Trans. Mag. **40**, 3443 (2004).
- ²³W. H. Press, S. A. Teukolsky, W. T. Vetterling, and B. P. Flannery, *Numerical Recipes in C: the art of scientific computing* 2nd ed. (Cambridge University Press, New York, 1992).
- ²⁴B. D. Cullity and C. D. Graham, *Introduction to Magnetic Materials* (Wiley, New Jersey, 2009).
- ²⁵R. Kubo, M. Toda, and N. Hashitume, *Statistical Physics II. Nonequilibrium Statistical Mechanics* (Springer-Verlag, Berlin, 1992).